Chapter- 5

5.1 Introduction

Raman spectroscopy is the technique of choice to study bio-molecules due to its water insensitivity and since most of the bio-molecules' activity is seen in their form of aqueous form. However, the inherently low signal output in Raman spectroscopy is the major stumbling block for their full-fledged applications in bio-molecules [1]. The discovery of Surface-enhanced Raman scattering (SERS), has resulted in a major fillip to study biological molecules using Raman spectroscopy [2]. SERS using semiconducting nanoparticles has proven to be a promising method for the detection of bio-molecules such as proteins, nucleic acids and neurotransmitters at low concentration level [3–5]. The SERS sensitivity of bio-molecules with respect to interaction at surface of semiconducting nanoparticles provides the insights to understand the behaviour and function of bio-molecules at molecular level, which play important role in the development of designing drugs, and associated diagnostic techniques [6].

We have investigated the SERS ability of bismuth heterostructure by considering organic pollutants. Further, to explore the potential application of bismuth material as SERS substrate for the detection of bio-molecules, we have considered two bio-molecules as acetylcholine (Ach), and Isatin. Acetylcholine is an important modulating neurotransmitter that transfers the signals from motor neurons to muscles, and many studies have been conducted regarding Ach's non-enzymatic hydrolysis which occurs in a basic media [7]. An uncontrolled drop in levels of Ach causes an imbalance or defects in motor coordinate and cognition, including learning and memory. The lack of concentration of Ach intensifies the Alzheimer's disease (AD) [8]. On the other hand,

Chapter- 5

Isatin (indole-2,3-dione) is an oxidized indole. It is abundantly present in body fluids, mammalian tissues, and in the brain of humans and animals [9]. Isatin has important role in the field of medicine due to its wide range biological, chemotherapeutic properties and pharmacological action (antimicrobial, anti-HIV, antiviral, antimalarial, anticancer etc.) [9]. In addition, urinary Isatin has been used as an endogenous marker in patients with Parkinson's disease as well as a biomarker of stress and anxiety. An innovative biological modulator raises the concentration of dopamine during stressful situations, which may contribute to the control of Ach levels in the brain. Isatin (10^{-4} M) administration increases acetylcholine levels in the brain region and its derivatives are used as therapeutic agents against Alzheimer's disease and the administration of dose of Isatin has significant effect on genes expression and Isatin binding proteins [10-11]. Neurochemical study underlying the effect of Isatin- induced acetylcholine release is still not well understood. Numerous methods have been employed for the quantitative detection of Isatin level such as spectrophotometry, fluorometry, enzymatic detection etc. [12–14], but they are time consuming besides requiring complicated experimental setups. Among the several experimental techniques SERS has been developed for rapid and accurate detection of low concentrations of neurotransmitters while a very few study has been done on Isatin using Raman and SERS spectroscopy [15–17]. Polat T et al. have reported the comparative experimental and theoretical study of 7-halogeno (-F, Br, CH_3) derivatives of Isatin by FT-Raman [15]. Similarly, Santhy et al. carried out both experimental and theoretical studies on the vibrational and electrical properties of 1-Phenylisatin [16]. Marin et al. have investigated the 5-nitroisatin and its complex with silver cation 1mM

using Raman and SERS [17]. However, quantitative analysis of Isatin using SERS has not yet received much attention despite its significance in biology.

In this work, Raman and Surface enhanced Raman study were performed to study the bio-molecules such as Isatin and its derivatives such as 1-Methylisatin (1-Misa), 1-Phenylisatin (1-Phisa), 5-fluoroisatin (5-Fisa), and 5-idoisatin (5-Iisa)) and another molecule acetylcholine on bismuth-based substrate. It is well recognized that substituted derivatives (R = NO_2, F, Cl, Br, I, CH_3, Ph) have been shown to be the most active substances with the relative biological activity [9,17]. Here, we present the first study on SERS spectra of Isatin and its derivative, and acetylcholine on bismuth substrate to the best of our knowledge. Moreover, pH dependent structural changes in Isatin containing molecules were performed because of its biological or medicinal importance and an attempt has been made to examine the interaction of Ach with Isatin molecules due its bio-complex formation using Raman spectroscopy.

5.2.1 Material and method

$Bi(NO_3)_3.5H_2O$ (SRL, India), Acetylcholine, Isatin, 1-Methylisatin (1-Misa), 5-Idoisatin (5-Iisa), 5-Fluoroisatin (5-Fisa), 1-Phenylisatin (1-Phisa), purchased from sigma-aldrich, ethanol, NaOH, HCl (Merck, India) and distilled water.

5.2.2 Synthesis of SERS substrate

Synthesis of Bismuth oxide was carried out using hydrothermal method as discussed in chapter 2 with the following modification in concentration of $Bi(NO_3)_3 \cdot 5H_2O$. 2 mmol of $Bi(NO_3)_3 \cdot 5H_2O$ was added in 30 mL ethylene glycol, and 25 mmol of urea was dissolved

in 20 ml distilled water. Both solutions were mixed with a constant stirring for 15 min after which the solution was transferred to an autoclave and kept for 24 h at 150 ^{0}C. The obtained precipitate ($Bi_2O_2CO_3$) was washed with ethanol and water three times and dried at 60 ^{0}C overnight. The product α-Bi_2O_3 was obtained via the calcination of $Bi_2O_2CO_3$ at 400 ^{0}C for 3h.

5.2.3 Raman and SERS measurement

Bio-molecules such as Isatin (10 mM to 1 mM) and its derivative 1-Misa (20 mM to 500μM), (20 mM to 1mM), 5-Iisa (10 mM to 500 μM), 5-Fisa (10 mM to 500 μM), 1-Phisa were analysed in ethanolic medium, and acetylcholine (10 mM to 500 μM) in aqueous solution. The prepared solutions of 20 μL analyte were mixed with the bismuth nanopaticles for 6 h. Raman and SERS spectrum of analytes were recorded using 785 nm diode laser as an excitation source with 76 mW, 5s integration time for Isatin and 10s for Ach. Moreover, WITec Raman intstrument with 532 nm and 633 nm wavelength was used to record the Raman spectrum of target molecules (1mW, 5s integration time at 532 nm, and 10 mW, 5s at 633 nm laser). In order to change the solution's pH value, NaOH solution and HCl acid were used. pH values were measured using pH paper.

5.2.4 Computational details

Vibrational frequencies were calculated using density functional theory (B3LYP) method at 6-311++G (d,p) basis set level for 1-Ph-AA, 5-Fisa, 5-F-AA, and 5-Iisa, and 5-I-AA at 3-21g basis set level of theory. Gaussian 09 package [19] was used to calculate the frequencies, and Gauss-View package was used for visualization. Potential energy

distribution (PED) analysis was done and the normal modes of vibration were assigned using the VEDA 4 program [20]. The prominent vibrational modes were used to assign the experimentally observed Raman frequency value.

5.3 Results and discussion

The formation of α-Bi_2O_3using the method described above was confirmed through XRD and Raman spectroscopy which was in good agreement with the results as discussed in Chapter 2 for α-Bi_2O_3 but the slight change in morphology.

5.3.1 SEM analysis

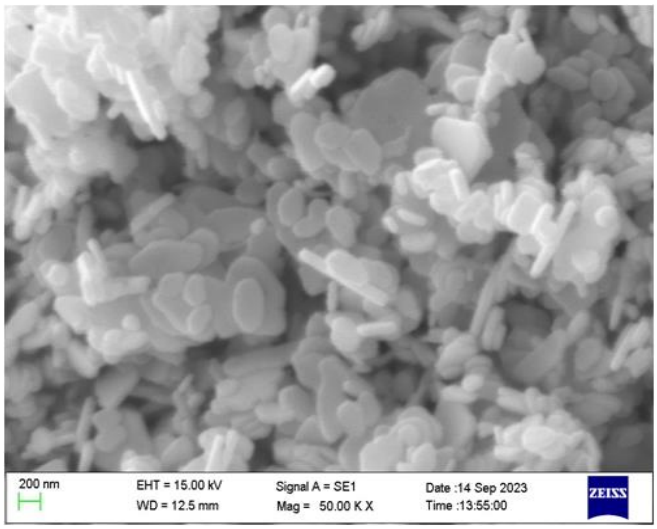

Figure 5.1 *SEM image of α-Bi_2O_3 nanoparticles.*

Scanning electron microscope image (SEM) shown in **Figure 5.1** depicts the ellipsoide like shape of the particles. The diameter size of the particles was in the range of 100-160 nm. This reveals that the size of as prepared α-Bi_2O_3 nanoparticles reduced from plate like structure to small ellipsoid like structure compared to the prepared materials

explained in chapter 2. The morphology and the small size of the nanoparticles have significant role in the SERS field.

5.3.2 pH dependent Raman study on Isatin and its derivative

The molecular structure of Isatin and its derivatives such as 1-Misa, 1-Phisa, 5-Fisa, and 5-Iisa molecules have orange or reddish color in solid state and change in color after addition of alkaline pH in solid or liquid state are shown in **Figure 5.2 (a)**. However the Isatin molecules can also exist in tautomeric form, and various studies show the influence of pH, solvent on keto-enol formation or oxidation of Isatin [21]. Moreover, the molecule is capable of changing its structure in reaction to external factors, such as pH change in the acidic or basic medium [22]. Effect of pH on Isatin and its derivative molecules were analysed through Raman spectrum at different laser source of 532, 633, and 785 nm to obtain the characteristic feature or spectral change with the change in Wavelength. Raman spectra of orange red ethanolic solution of 0.1M Isatin and its derivative at acidic medium pH $\leq$ 6 or at basic medium pH $\geq$ 8 are shown in **Figure 5.2 (a)-(f).** Raman spectra of Isatn's at pH $\geq$ 8 demonstrates the remarkably different structure or at highly alkaline pH 12, for instance, changes in structures were observed. **Figure 5.2 (b)** shows the Raman spectrum of Isatin in solid state and in alkaline medium. The structural transformations were characterised by the most prominent peaks at 1546, and 1482 cm^{-1} corresponds to the C=C stretching, and another peaks at 1417, 1345 cm^{-1} assigned to C-C stretching of anthranilic acid (AA) with 532 nm laser. Moreover, the transformation of Isatin into AA was also observed with the appearance of the peak at 1727 cm^{-1} for Isatin molecules termed as Isatin+AA spectrum at 633 and 785 nm due to the high proportion of Isatin in

mixture. The vibrational modes of observed molecule after hydrolysis are in good agreement with the previously reported results in the literature [22-24]. The detailed assignment corresponding to the characteristic peaks are given in **Table 5.1.**

Similarly,1-Misa, 1-Phisa, 5-Fisa, 5-Iisa molecules with the addition of basic pH ≥ 8 were transformed into 1-M-AA (1-Methyl anthranilic acid), 1-Ph-AA (1-Phenyl anthranilic acid), 5-F-AA (5-Fluoro anthranilic acid), 5-I-AA (5-Ido anthranilic acid) as depicted in **Figure 5.2 (c)**, **Figure 5.2 (d)**, **Figure 5.2 (e)**, **Figure 5.2 (f)**, and their tentative assignments are listed in **Table 5.2**, **Table 5.3**, **Table 5.4**, **Table 5.5**, respectively. In the Raman spectrum shown in **Figure 5.2 (c),** in basic medium the sharp peak of 1-Misa at 1734 cm^{-1} was disappeared and new peaks of 1-M-AA were observed at 1628 cm^{-1} which attributed to the stretching mode of C-C and another characteristic peak at 1521 cm^{-1} corresponds to the C-C stretching and bending mode of CHC [25]. The Raman spectrum was recorded at different excitation source shows the appearance of distinct spectral modes of the molecule as shown in **Table 5.2**. The observed results clearly suggest the complete transformation of 1-Misa into 1-M-AA compared to the Raman spectrum of 1-Misa in solid state. In case of 1-Phisa, Raman spectrum were observed at 532 in solid state shows all characteristic peaks as compared to and 785 nm (**Figure 5.3 (a)**), while at 633 nm there was no significant peaks (which was not shown in the Figure). 1-Phisa in basic medium shows sharp and strong peaks at all considered wavelength as displayed in **Figure 5.2 (d)** and the major change in the spectrum can be seen in the region of 1600 cm^{-1}. Another changes were observed peaks for 1-Ph-AA at 1321 cm^{-1} ascribed to the C-C, N-C stretching and 1418 cm^{-1} attributed to the C-C stretching and HCC bending in

ring. Likewise, the obtained results at different laser for 5-Fisa and 5-Iisa are shown in **Figure 5.2 (e) and Figure (f)** and the change in structure into 5-F-AA and 5-I-AA due basic pH are highlighted through the major peaks in their respective spectrum and their assignment via DFT method are shown in table. Moreover, we observed that the changed structure of Isatin and its derivatives in basic medium were re-stabilized in its original state in acidic medium.

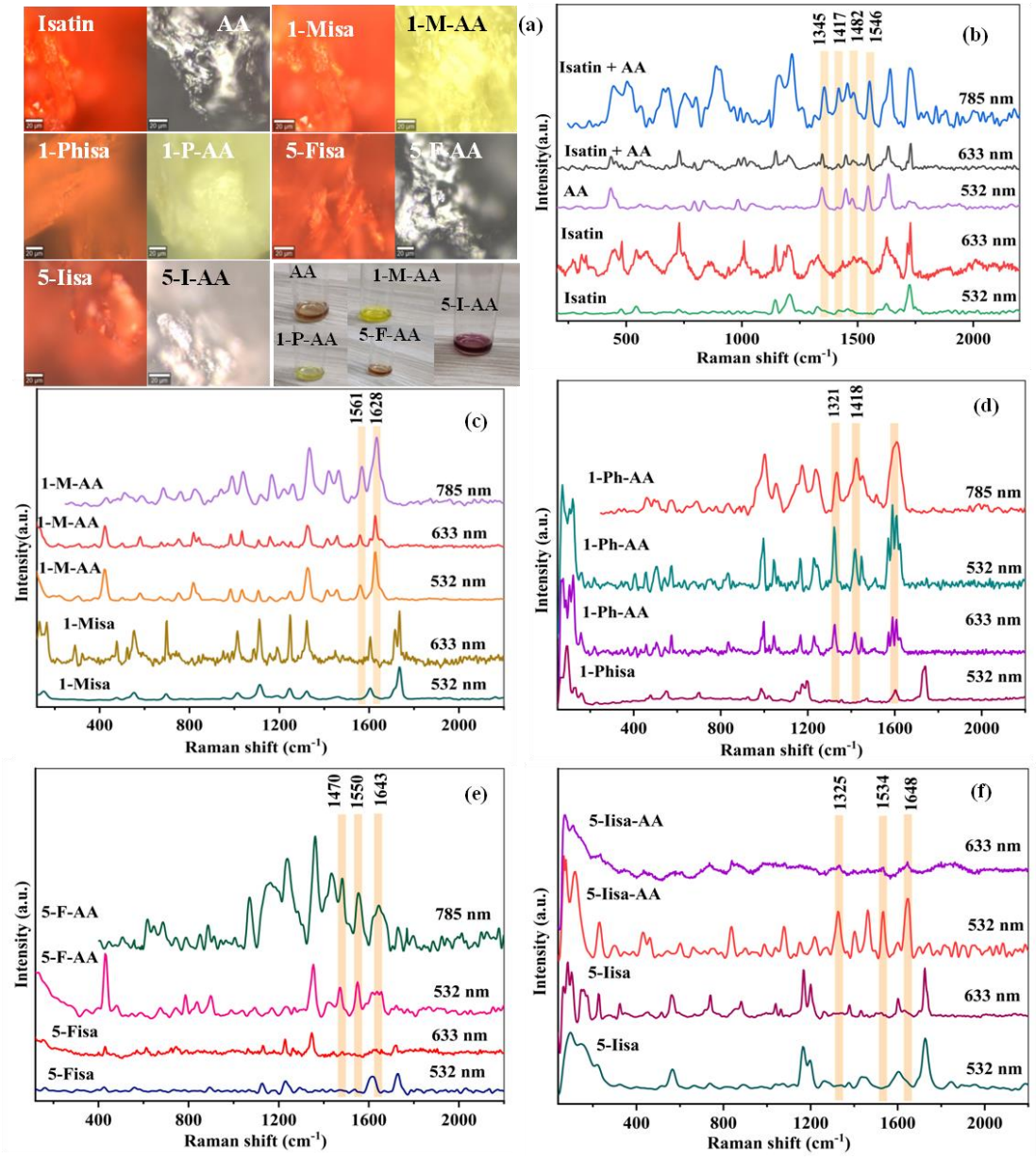

Figure 5.2 (a) *topography image of Isatin and its derivates with change in color. Raman spectrum in acidic and basic medium for (b)Isatin (c) 1-Misa (d) 1-Phisa (e) 5-Fisa (f) 5-Iisa.*

5.3.3 SERS measurement of Isatin and its derivatives

The SERS analysis was performed at 785 nm laser source for all selected molecules.

Figure 5.3 (a) shows the normal Raman spectrum of solid of Isatin. Derivates of Isatin were also subjected to Raman measurements to compare the enhancement of Raman signal after the adsorption of the considered analyte on bismuth nanoparticle SERS substrate.

Figure 5.3 (b) shows the Raman spectrum of powder Isatin, and **Figure 5.3 (c)** shows the SERS spectrum with the signature peaks at 726, 950, 1009, 1146, 1209, 1420, 1625, and 1727 cm^{-1}, and their vibrational modes are illustrated in **Table 5.1**. α-Bi_2O_3 nanoparticles was used as SERS substrate to demonstrate the SERS activity of Isatin. The most intense peak at 1727, and 1209 cm^{-1}corresponds to the Raman mode of C=O stretching, and N-H bending. The obtained SERS results are in good agreement with previous results [23]. The detection limit was found to be as low as 800 μM. According to the previous report the lowest detection limit for Isatin (5-nitroisatin) was determined to be 1mM on silver nanoparticles which demonstrate that α-Bi_2O_3substrate exhibits good SERS activity for the detection of Isatin.

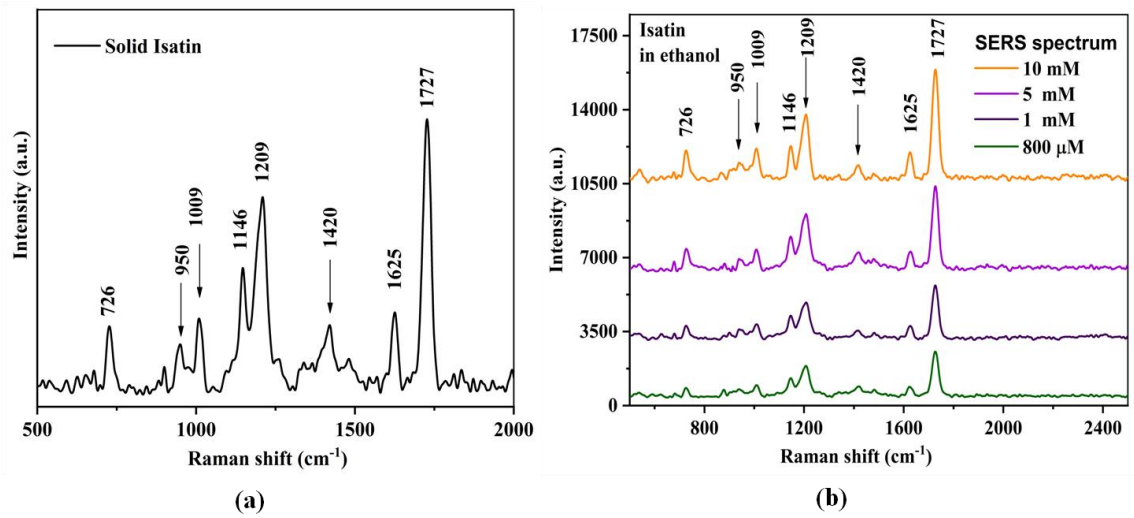

Figure 5.3 *(a) Raman spectrum of solid Isatin, and (b) SERS spectrum of Isatin on α-Bi_2O_3 substrate from 10 mM to 800 µM.*

Figure 5.4 (a) shows the Raman peaks of solid 1-Misa at 479, 520, 548, 695, 876, 896, 950, 1014,1112, 1155, 1191, 1246, 1322, 1457, 1606, 1716, and 1734 cm^{-1}. **Figure 5.4 (b)** shows the SERS spectrum of 1-Misa on α-Bi_2O_3 and the characteristic peaks match well with the solid Raman spectrum shown in **Table 5.2**. In the SERS spectrum a new peak appeared at 1061cm^{-1}can be assigned to C-C stretching mode may be arises due to the interaction of 1-Misa with α-Bi_2O_3 substrate. The all SERS peaks are well agreed with the previous reported frequencies [15]. The lowest detection limit was 800 µM.

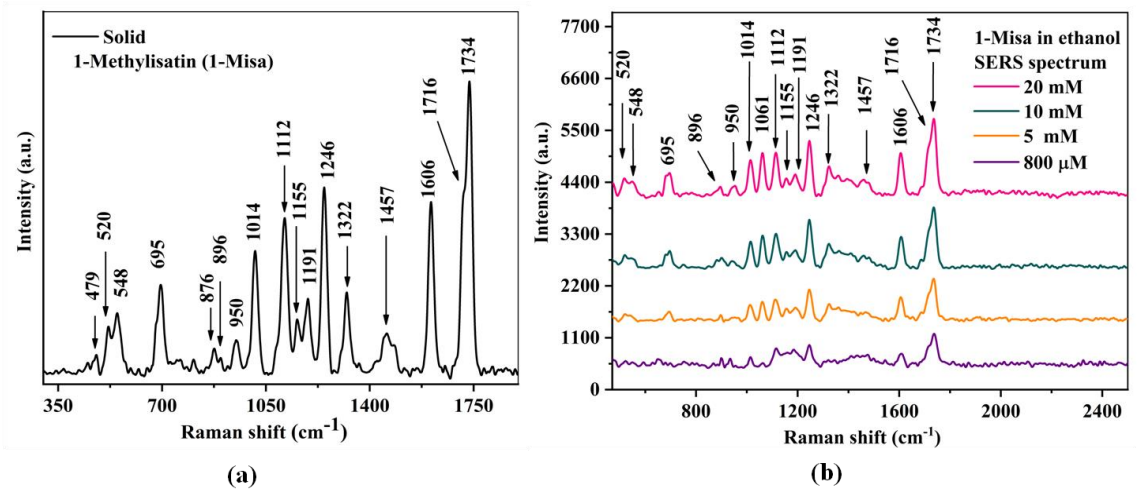

Figure 5.4 *(a) Raman spectrum of solid 1-Misa (b) SERS spectrum of 1-Misa on α-Bi_2O_3 substrate from 20 mM to 800 µM.*

Raman spectrum of solid 1-Phenylisatin (1-Phisa) is shown in **Figure 5.5 (a)** and the assignment of their characteristic peaks at 992, 1155, 1178, 1197, 1366, 1601, and 1739 cm^{-1} are listed in **Table 5.3**. **Figure 5.5 (b)** shows the SERS spectrum of 1-Phisa on bismuth substrate where the characteristic peaks were observed at 697, 750, 793, 992, 1023, 1155, 1178, 1197, 1303, 1358, 1601, and 1739 cm^{-1}, indicating enhancement in Raman signal of 1-Phisa on bismuth substrate due to the adsorption as compared to the solid Raman spectrum. The sharp peak at 1739 and the peak at 1601 cm^{-1} corresponds to the C=O stretching bond, and C-C stretching, C-H bending. Another most intense peak at 1197 cm^{-1} can be assigned to C-N or C-H stretching, and 992 cm^{-1} due to C-C stretching. The lowest detection limit for 1-Phisa was determined to be 15 mM to 1mM.

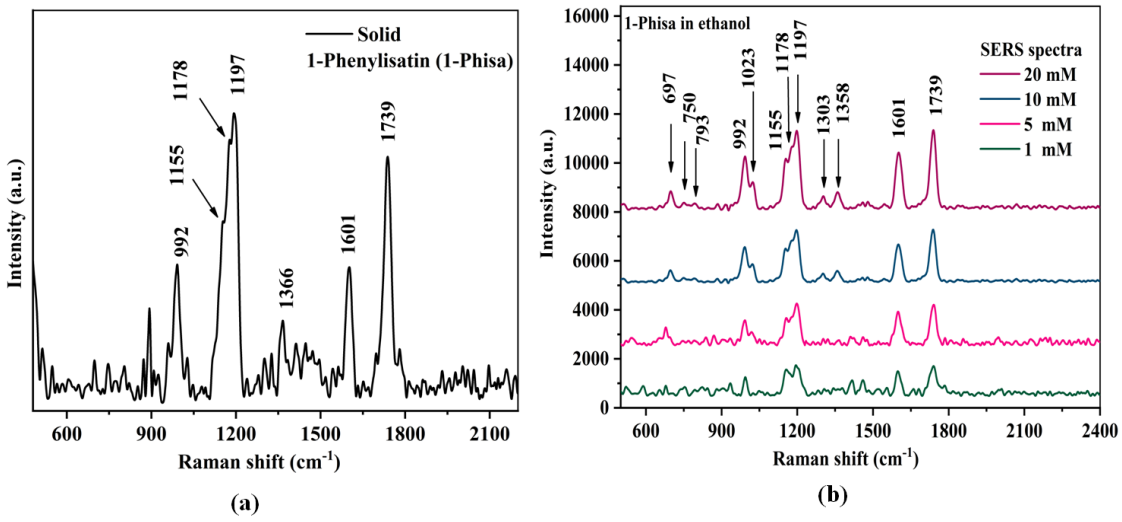

Figure 5.5 *Raman spectra of (a) solid 1-Phisa and (b) SERS spectrum of 1-Phisa on bismuth substrate from 20 mM to 1mM.*

Figure 5.6 (a) display the Raman spectrum of 5-Fisa. The Raman peaks were observed at 1231, 1618, and 1727 cm^{-1}. The intensity of Raman peaks increases after the adsorption of 5-Fisa on α-Bi2O3 substrate compared to normal Raman spectrum as shown in the SERS spectrum **Figure 5.6 (b)**, and their assignment are listed in **Table 5.4**. In the SERS spectrumthe most intense peaks were observed at 1242, and 1738 cm^{-1} due to C-H in plane bending vibration and C=O stretching, respectively. The appearance of new some peaks at 501, 558, 737, 791, 900, 982, 1093, 1122, 1407, 1480, 1622 and 1704 cm^{-1} reveals the adsorption of 5-Fisa on bismuth oxide, which are well agreed with the previous reported 7-FluoeroIsatin Raman data [15]. Further their vibrational frequecinces validated theoretically at B3LYP/6-311++G(d,p) level of theory. The lowest detection limit was found to be 500 μM.

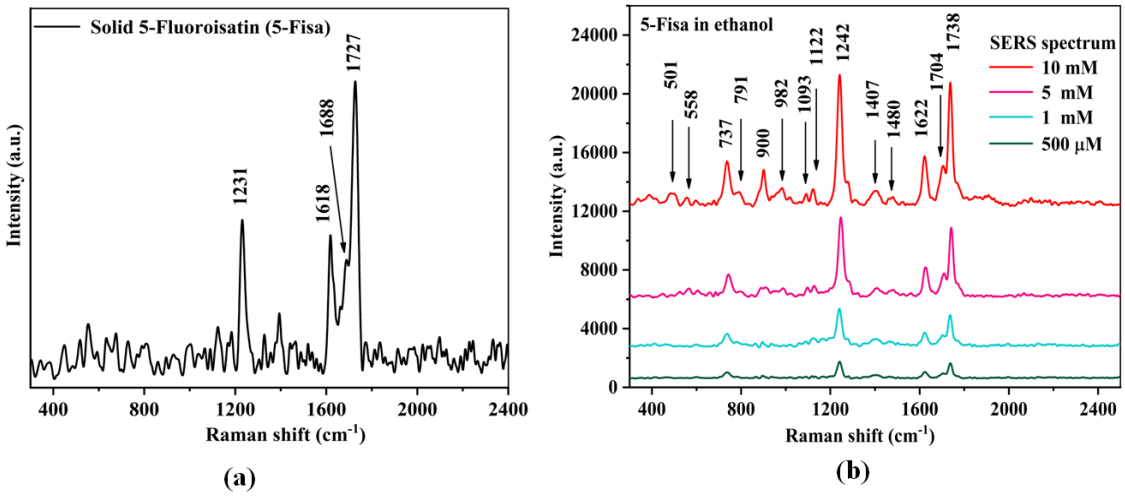

Figure 5.6 *(a) Raman spectrum of pure 5-Fisa, and SERS spectrum of 5-Fisa on α-Bi_2O_3substrate from 10 mM to 500 μM.*

Raman spectrum of solid 5-idoisatin or 5-Iisa demonstrates the characteristic peaks at 1166, 1194, 1377, 1429, 1601 and 1727 cm^{-1} as shown in **Figure 5.7 (a)**, and the SERS peaks observed at 501, 558, 737, 791, 900, 982, 1093, 1122, 1407, 1480, 1622, 1704, and 1738 cm^{-1} are shown in **Figure 5.7 (b)**, and the assignment are shown in **Table 5.5**. The sharp peaks at 1727, and 1166 cm^{-1} corresponds to the C=O stretching and C-N stretching vibration. Experimentally observed frequencies are well supported by the predicted frequencies at B3LYP/3-21G level of theory.

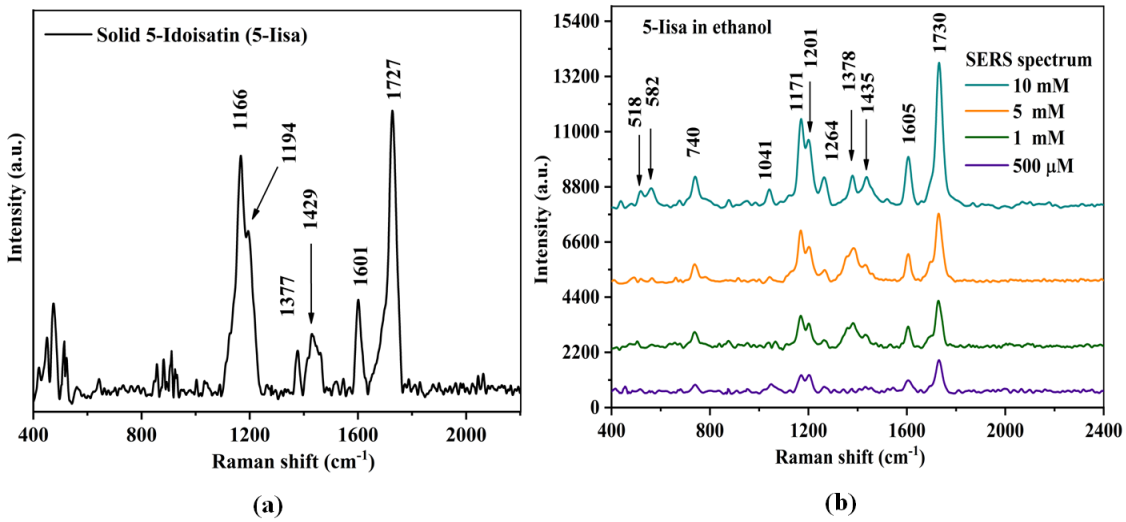

Figure 5.7 *(a)Raman spectrum of solid 5-Iisa, and (b)SERS spectrum of 5-Iisa on α-Bi_2O_3substrate at different concentration from 10 mM to 500 μM.*

5.3.4 pH dependent Raman and SERS study on acetylcholine (Ach)

Figure 5.8(a) depicts the Raman spectra of aqueous Ach (0.35M) at different pH values. According to the literature environmental conditions, such as pH, solvents or the surface properties of metals, have an impact on Raman modes of neurotransmitters via chemical process [26]. To analyse these effect precisely we have first recorded the Raman spectra of Ach neurotransmitter with different laser source for comparison. At pH < 7 or in acidic medium the characteristic peaks of Ach were observed at both 532 nm (**Figure 5.8 a (i)**) as well as at 633 nm laser (**Figure 5.8 a (ii)**) with slight decrease in intensity at peak 1730 cm^{-1} compare to 532 nm. On the other hand, hydrolysis process of Ach was observed in basic medium with the increase in pH > 7 or = 9 -12 (from **Figure 5.8 a (iii)-(vi)**) resulting product were choline and acetate ion. The intensity of Raman peaks at 635 (acetyl part), and 870 cm^{-1} (choline part) significantly decreases but the peaks at 825, and 1730 cm^{-1} (acetyl part) vanished at pH > 9, while the peaks intensity at

760, 1337, 1414 cm^{-1} considerably increases. A new peak was observed at 921 cm^{-1} due to the stretching vibration of C-C of acetate ion which intensity increases with increase in hydrolysis. The Raman modes in the range of 2800-3100 cm^{-1} do not show any significant change. These observed results are consistent with the previous report [26] and the details of Raman peaks and their assignment are given in **Table 5.6**.

5.3.5 Interaction of Isatin and its derivative with Ach

It was observed that Isatin considerably increases the acetylcholine level in rat brain. To obtain the detail how Isatin interact with Ach, we present the analysis of Isatin with Ach using Raman spectra at 532 nm laser as shown in **Figure 5.8 (b)**. 0.35 M aqueous Ach, and 0.05 M ethanolic Isatin were mixed at different pH values. In the mixture of Isatin + Ach, Raman spectrum display the characteristic peaks of Isatin at 1613, 1144, 1193, 543, and 470 cm^{-1}, the sharp peaks at 3026, 2974, 2934, 2818, 1446, 1268, 1051, 945, 872, 821, 711, and 635 cm^{-1} were observed for Ach. The observed spectral features can be used to distinguished the neurotransmitter and Isatin. There are some overlapping peaks close to 1735, 1333, and 1005 cm^{-1}, the intensity of the Raman peak increases at 1735 cm^{-1}. A new peak at 2246 cm^{-1} assigned to bending mode of O-H was appeared in acidic medium at pH > 7 may arises due to the tautomeric form of Isatin. In addition, as pH increases from acidic to basic medium, due to the structural change in Isatin as discussed in section 5.3.2, the slight shift in peak positions by 8 cm^{-1} and the change in Raman features of Isatin + Ach were observed as illustrated in **Figure 5.8 (b)**.

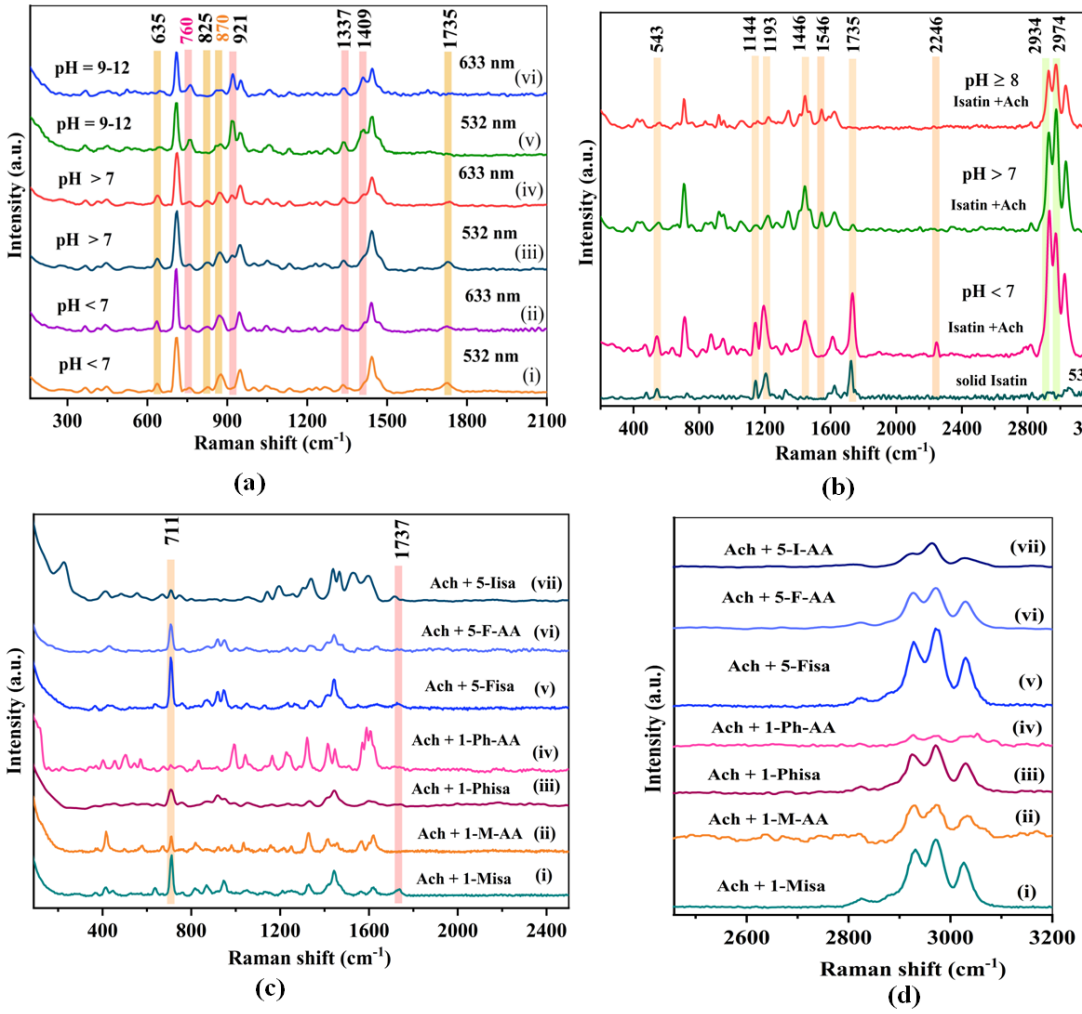

Figure 5.8 *(a) Raman spectra of Ach with different pH at different laser source (b) Ananlysis of Ach with Isatin in acidic and basic medium (c) mixture analysis of Ach with derivatives of Isatin and (d) mixture analysis in the 2800 to 3200 cm^{-1} range.*

At pH ≥ 8 multivibrations of AA were observed in the mixture of Isatin + Ach, which reveals that after hydrolysis Ach can interact with AA instead Isatin and can be used as biomarker for the disease detection. Moreover, Raman spectra in the range of 2800- 3100 cm^{-1} show the variation in peak intensity in basic medium as compared to acidic medium at 2934, and 2974 cm^{-1} due to the stretching bond of $(CH_3)N$, and asymmetric stretching

of CH_2.

Similarly, mixture analysis of Ach with Isatin derivatives such as 1-Misa, 1-Phisa, 5-Fisa, and 5-Iisa as well as its structural changes were performed with the constant peak at 711 cm^{-1} of Ach and other characteristic peaks as shown in **Figure 5.8 (c). Figure 5.8 (d)** shows the spectral change in the region of around 3000 cm^{-1} this can be due to the interaction of Ach with Isatin derivatives.

5.3.6 SERS study of Ach on bismuth oxide

Raman spectrum of acetylcholine (Ach) is shown in **Figure 5.9 (a)** and their vibrational modes are given in **Table 5.6**. The SERS spectrum of Ach is illustrated in **Figure 5.9 (b)** with concentration ranging from 10 mM to 1mM in aqueous medium at pH > 7. The prominent peaks were observed at 708, and 1446 cm^{-1} can be assigned to symmetric stretching mode of N-C in $(CH_3)N$ and asymmetric bending mode of CH_3 group of choline part, respectively [27]. SERS peaks at 1129 cm^{-1} due stretching of C-C bond, and at 3027 cm^{-1} due asymmetric mode of $(CH_3)N$ were red shifted by 18 cm^{-1} and blue shifted by 9 cm^{-1}, respectively compared to the Raman spectrum of the solid Ach. Intensity of the both peaks at 918 and 1409 cm^{-1} increases due to the adsorption of Ach on α-Bi_2O_3 nanoparticles, which correspond to the asymmetric stretching, and bending mode of $(CH_3)N$, respectively. The obtained results match well with the literature [26–28].

Figure 5.9 (c), and **(d)** shows the pH dependent SERS study of 5 mM Ach on α-Bi_2O_3 at 785 nm excitation source in aqueous and ethanolic medium at different pH solution. In **Figure 5.9 (c)** CH_3 bending and C-C stretching mode assigned at 1056 cm^{-1} is strong at pH > 7 increases towards pH ≥ 9 in aqueous solution, gleaned by the intensity ratio I_{918}/I_{1050} which increases from 2.0 to 4.0, respectively, and the new peak corresponding to acetate ion (CH_3COO^-) appears at 1544 cm^{-1} after hydrolysis. As shown in **Figure 5.9 (d)**, we observed that the intensity of SERS spectral features of ethanolic Ach are decreases at alkaline pH 12 in ethanolic medium as compared to aqueous medium, and is more likely shifted by 10 cm^{-1} at peak 1349 cm^{-1} compared to the aqueous Ach, and this can be attributed to the bending mode of CH_2. In contrast to aqueous Ach, the peak appeared at 882 cm^{-1} increases with pH value > 9, which can be assigned to symmetric stretching mode of C-N, while the peak at 1735 cm^{-1} disappeared in both mediums associated with the stretching mode of C=O. Therefore, the results suggest that environmental parameters affect the structure of Ach neurotransmitter.

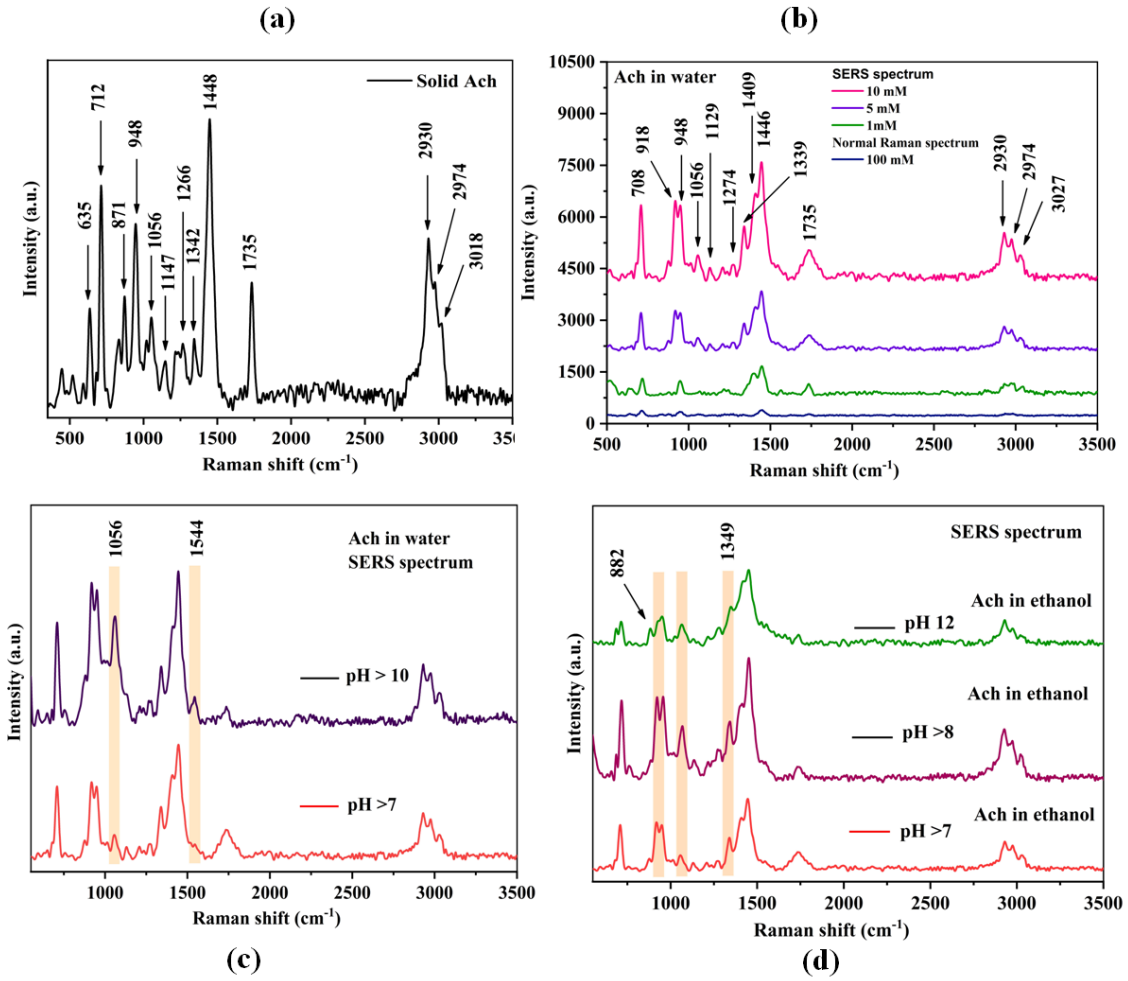

Figure 5.9 *(a) Raman spectrum of solid Ach (b) SERS spectrum of Ach on α-Bi2O3 substrate from 10 mM to 1mM (c) & (d) SERS spectra of Ach in aqueous and ethanolic medium at different pH value.*

5.4 Conclusion

In summary, we successfully prepared α-Bi_2O_3 nanoparticles and used as SERS substrate for the detection of bio-molecules. Raman study of Isatin and its derivative shows the structural change in basic medium. The SERS detection of Isatin on bismuth oxide were observed with the lowest detection limit for Isatin and 1-Misa was 800 μM, for 1-Phisa it was 1mM, and for 5-Fisa or 5-Iisa was 500 μM. Further, the hydrolysis of acetylcholine was observed in SERS, which reveals change in acetyl and choline part of Ach and the interaction of Ach with Isatin can play important role in medical field. The lowest detection limit was found to be 1mM for Ach. pH dependent Raman study of Isatin and its structural change demonstrate that it can losses its original properties and can interact with other biological species.

Table 5.1 Tentative assignment for Raman frequencies (cm^{-1}) of Isatin, AA, and Isatin + AA

Isatin					**AA**	**Isatin + AA**		
Raman			**SERS**	**Assignment**	**Raman**	**Raman**		**Assignment**
532 nm	**633 nm**	**785 nm**	**785 nm**	**Ref [23]**	**532 nm**	**633 nm**	**785 nm**	**Ref [24]**
					3348			ϒNH
					3042, 3019		2410	ϒCH
1728	1728	1731	1727	ϒC=O		1730	1727	
	1715					1714		
1624	1624	1629	1625	ϒC=C	1632	1634	1641	δNH
1593				δNH	1609	1613	1613	ϒCC
		1420	1420	ϒC-C	1546	1546	1552	ϒC=C
1325	1325			cCN	1482	1482	1482	ϒC=C
1206	1206	1212	1209	ϒCN	1450	1450	1456	ϒC=C
1143	1143	1149	1146	δCH		1417	1417	
1009	1009	1015	1009	δCH		1345	1350	ϒCC
			950	φCH		1200	1216	δN-H
730	730	733	726	φCH		1147	1154	
542	544			δCCC	983		1015	δCH
482	482			φCCC	838			φCH
					794	730	735	δCH
						454, 434		
					434			φCNH

Table 5.2 Tentative assignment for Raman frequencies (cm^{-1}) of 1-Misa, and 1-M-AA

1-Misa					**1-M-AA**		
Raman			**SERS**	**Assignment**	**Raman**		**Assignment**
532 nm	**633 nm**	**785 nm**	**785 nm**	**Ref [15]**	**532 or 633 nm**	**785 nm**	**Ref [25]**
3058				νCH benzen ring	3342		νNH
3029				νCH benzen ring	3068		νCH
2944				ν_{as} CH_3 (C-H)	2997		$\nu_{as}CH_3$
1734	1734	1734	1734	ν C-O	2930		$\nu_{as}CH_3$
1715	1715	1716	1716	νC-O	2901		$\nu_{as}CH_3$
1605	1605	1606	1606	νCC benzen ring	2861		ν_sCH_3
1478	1478	1481		ρCH_2 of CH_3, δCH_2	2811		
1454	1449	1457	1457	αCH3	1653		νCO
1321	1321	1322	1322	δCCH	1628	1633	νCC
1247	1247	1246	1246	ν CN, δCCH	1606		νCC
1189	1189	1191	1191	νCC	1558	1567	νCC, δCHC
	1158	1155	1155	δCCH	1457	1463	$\delta_{as}CH_3$
1114	1110	1112	1112	ν CC, δCCH	1414	1419	δ_sCH_3
	1087		1061	ν CN	1328	1334	δCHC, νCN
1013	1013	1014	1014	ν CC benzen ring	1250	1260	δCHC, νCC
954	950	950	950	ν CC, δCCO	1214	1221	δCHC
		896	896	δCCC	1158	1165	δCHC
		876			1107	1117	ρCH_3
		806		ϒOCCO	1033	1038	νCC
694	699	695	695	ν CC, δCCC	985	990, 941	
551	553	548	548	δCCC	842, 818	824	
		520	520	δCCN	753, 702	760	
475	476	479		ν CC	675, 581	683	
	290			δCCO, δN-CH_3	501, 422	588, 512	
152	164			τCH_3	379, 306	430	
	131			τCH_3	216		

Table 5.3 Tentative assignment for Raman frequencies (cm^{-1}) of 1-Phisa, and 1-Ph-AA

1-Phisa				**1-Ph-AA**		
Raman		**SERS**	**Assignment**	**Raman**		**Assignment**
532 nm	**785 nm**	**785 nm**	**Ref [16]**	**532 nm**	**785 nm**	**B3LYP/6-311++G (d,p)**
3078			ν CH	3279		ν NH
3050			ν CH + ν CC3	3088		ν CH
3023			ν CH	3055		ν CH
1737	1739	1739	ν C = O, δCN	1626		ν C = O
1601	1601	1601	ν C C, δCH	1608	1610	ν CC
1470	1366	1358,1303	ν C C, δCH	1590		ν CC
1197	1197	1197	δCH, ν C N	1571		ν CC
1173	1178	1178	ν C N	1508	1515	ν NC, δHNC
1148	1155	1155	δCH	1446	1451	δ HCC
1022		1023	δCH	1417	1424	νCC, δHCC
988	992	992	δ ring,ν CC	1321	1333	ν CC, ν NC
924			ϒCH2	1244	1236	δ HCC
		793	ϒring1	1228		ν CC, δ HCC
		750	ϒring, ϒring1	1166	1174	ν NC
702		697	ϒring1	1043	1054	νOC, ϒCCC
552			ϒring, ϒring2	999	1002	τHCCC
480			ϒring1	836	835	τHCCC
232			ϒring	738		νCC,ϒCCC
161			ϒring, δ ring	574		δ CCC
133			ϒring2	544		τHOCC
				503, 457		τCCCC
				407		τCCCC
				372, 344		ν CC, δ CCC
				219		ϒNCC, τCCCC
				157		δCCC
				121, 105		τCCCC
				88		τCCCC
				75		ϒNCC

Table 5.4 Tentative assignment for Raman frequencies (cm^{-1}) of 5-Fisa, 5-F-AA, and 5-Fisa+5-F-AA

5-Fisa				5-F- AA	5-Fisa + 5-F-AA		Assignment
Raman		SERS	Assignment	Raman	Raman		
532 nm	785 nm	785 nm	B3LYP/6-311++G (d,p)	532 nm	633nm	785 nm	B3LYP/6-311++G (d,p)
1726	1727	1738	ν OC		1722	1727	ν OC
	1688	1704	ν OC				
1617	1618	1622	ν CC	1643			ν CC
		1480	δHCC, ν CC ring	1550		1554	ν CC
		1407	δ HCC, ν CC	1470		1480	δHCC
1292			δHCC, ν CC, νCN	1422		1431	ν CC
1230	1231	1242	δHCC, νCF, ν CC		1346	1418	ν CC
1181			ν CC, ν CN	1353	1230	1360	ν CC
1127		1122	νNC, δ HCC		1177	1237	νFC, δHCC
		1093	δHCC, ν CC ring		1130	1162	δHOH, δCCC
		982	ϒHCCH, ϒCCCH		1070		δHCC
894		900	ν CC, δ CCO, ν CN			1070	νCO
		791	ϒCCCH	898			τHCCN
		737	ϒCCCC, ϒCCCH	838	786		τHCCN
560		558	ν CC, δ CCF	786	743		δCCC, νCN
425		501	δ CCC	742	676		τCCCC
161			τCCCC, τCNCC	676	614		δOCO, δCCC
				479	429		τHCCN, τCCCC
				430			τHNCC

Table 5.5 Tentative assignment for Raman frequencies (cm^{-1}) of 5-Iisa, and 5-I-AA

5-Iisa					5-I-AA		
Raman shift (cm^{-1})			SERS	Assignment	Raman		Assignment
532 nm	633 nm	785 nm	785 nm	B3LYP/3-21G	532 nm	633 nm	B3LYP/3-21G
1726	1726	1727	1730	νOC	1648	1648	νCC, ϒHNH
1605	1600	1601	1605	νCC	1601		νCC, ϒHNH
1434	1434	1429	1435	νCC	1534	1534	νOC, νCC, ϒHNH
1374	1379	1377	1378	δHNC, δHCC	1462		δHCC
1264	1264		1264	νCC, δHNC	1402		ν CC
1197	1200	1194	1201	νCC, δHCC	1325	1325	δHCC
1164	1166	1166	1171	νCC, δHCC	1218		ν CC, δHCC, ν NC
	1062			νCC	1152		δHCC
	1039		1041	νCC	1077		ν CC, δHCC
889	880			δCCC, νNC	988		τHCCN
738	859			τHCCC	838	838	ϒCCC
	741		740	τCCCC	601		ϒCCC
565	562		582	τHNCC	461, 430		τHNCC
	451		518	νNC, τHCCC, τCCCC	301		τCCCC
324	325			τCNCC, τCCCC	232	232	ν IC
218	225			δOCC	119, 76	108	δCCC, δICC
147	157			τCNCC			
95	102, 85, 65			δOCC			

Table 5.6 Tentative assignment for Raman frequencies (cm^{-1}) of Ach

Ach			
Raman		**SERS**	**Assignment**
532 or 633 nm	**785 nm**	**785 nm**	**Ref [26-28]**
3029	3018	3027	$\nu_{as}(CH_3)N$
2974	2974	2974	$\nu_s(CH_3) + \nu_s(CH_2)$
2934	2930	2930	$\nu_s(CH_2)$
2821			$\nu_s(CH_3)$
1726	1735	1735	ν (C=O)
		1544	$\delta(CH_2)$
1467			δ(HCH)
1442	1448	1446	$\delta_{as}(CH_3)$
		1409	$\delta(CH_3)N$
1333	1342	1339	$\delta(CH_2)$
1271	1266	1274	$\omega_{as}(CH_3)$
1230			
1204	1147		τHCNC
1129		1129	ν (C-C) + τHCNC
1075	1056	1056	ν (C-C) + $\delta(CH_3)$
1046			τHCNC + ν_s (O-C)
1000			
950	948	948	ν (N-C) +δ (HCN)
		918	$\nu_{as}(CH_3)N$
870	871	882	ν_s (N-C)
825			τHCCO
760			ν_s (N-C)
711	712	708	ν_s (N-C)
635	635		ν (C-C) + $\delta(COO^{-})$
441			Υ(OCOC) + δ (CNC)
413, 366			δ (CCO) + δ (CNC)

References:

[1] S. Siddhanta and C. Narayana, "Surface enhanced Raman spectroscopy of proteins: implications for drug designing," *Nanomater. Nanotechnol.*, vol. 2, p. 1, 2012.

[2] J. Kneipp, H. Kneipp, and K. Kneipp, "SERS—a single-molecule and nanoscale tool for bioanalytics," *Chem. Soc. Rev.*, vol. 37, no. 5, pp. 1052–1060, 2008, doi: 10.1039/B708459P.

[3] X. Wang, N. Choi, Z. Cheng, J. Ko, L. Chen, and J. Choo, "Simultaneous detection of dual nucleic acids using a SERS-based lateral flow assay biosensor," *Anal. Chem.*, vol. 89, no. 2, pp. 1163–1169, 2017.

[4] A. Musumeci *et al.*, "SERS of semiconducting nanoparticles (TiO2 hybrid composites)," *J. Am. Chem. Soc.*, vol. 131, no. 17, pp. 6040–6041, 2009.

[5] R. Haldavnekar, K. Venkatakrishnan, and B. Tan, "Non plasmonic semiconductor quantum SERS probe as a pathway for in vitro cancer detection," *Nat. Commun.*, vol. 9, no. 1, p. 3065, 2018.

[6] H. K. Lee *et al.*, "Designing surface-enhanced Raman scattering (SERS) platforms beyond hotspot engineering: emerging opportunities in analyte manipulations and hybrid materials," *Chem. Soc. Rev.*, vol. 48, no. 3, pp. 731–756, 2019.

[7] K. B. Schowen, E. E. Smissman, and W. F. J. Stephen, "Base-catalyzed and cholinesterase-catalyzed hydrolysis of acetylcholine and optically active analogs," *J. Med. Chem.*, vol. 18, no. 3, pp. 292–300, Mar. 1975, doi: 10.1021/jm00237a017.

[8] D. Fu, W. Yang, and X. S. Xie, "Label-free Imaging of Neurotransmitter Acetylcholine at Neuromuscular Junctions with Stimulated Raman Scattering," *J. Am. Chem. Soc.*, vol. 139, no. 2, pp. 583–586, Jan. 2017, doi: 10.1021/jacs.6b10727.

[9] P. Naumov and F. Anastasova, "Experimental and theoretical vibrational study of isatin, its 5-(NO2, F, Cl, Br, I, CH3) analogues and the isatinato anion," *Spectrochim. Acta Part A Mol. Biomol. Spectrosc.*, vol. 57, no. 3, pp. 469–481, 2001.

[10] N. Hamaue *et al.*, "Isatin, an endogenous MAO inhibitor, as a new biological modulator," *CNS Drug Rev.*, vol. 5, no. 4, pp. 331–346, 1999.

[11] N. Hamaue *et al.*, "Comparative study of the effects of isatin, an endogenous

MAO-inhibitor, and selegiline on bradykinesia and dopamine levels in a rat model of Parkinson's disease induced by the Japanese encephalitis virus," *Neurotoxicology*, vol. 25, no. 1–2, pp. 205–213, 2004.

[12] M. Sobaszek, K. Siuzdak, J. Ryl, R. Bogdanowicz, and G. M. Swain, "The electrochemical determination of isatin at nanocrystalline boron-doped diamond electrodes: Stress monitoring of animals," *Sensors Actuators B Chem.*, vol. 306, p. 127592, 2020, doi: https://doi.org/10.1016/j.snb.2019.127592.

[13] K. Mawatari, M. Segawa, R. Masatsuka, Y. Hanawa, F. Iinuma, and M. Watanabe, "Fluorimetric determination of isatin in human urine and serum by liquid chromatography postcolumn photoirradiation," *Analyst*, vol. 126, no. 1, pp. 33–36, 2001.

[14] S. Manabe, Q. Gao, J. Yuan, T. Takahashi, and A. Ueki, "Determination of isatin in urine and plasma by high-performance liquid chromatography," *J. Chromatogr. B Biomed. Sci. Appl.*, vol. 691, no. 1, pp. 197–202, 1997.

[15] T. Polat, F. Bulut, I. Arıcan, F. Kandemirli, and G. Yildirim, "Vibrational assignments, spectroscopic investigation (FT-IR and FT-Raman), NBO, MEP, HOMO–LUMO analysis and intermolecular hydrogen bonding interactions of 7-fluoroisatin, 7-bromoisatin and 1-methylisatin – A comparative study," *J. Mol. Struct.*, vol. 1101, pp. 189–211, 2015, doi: https://doi.org/10.1016/j.molstruc.2015.08.033.

[16] K. R. Santhy, M. D. Sweetlin, S. Muthu, M. Raja, and C. S. Abraham, "Optical, vibrational (FT-IR and FT-Raman), electronic and molecular docking investigations of 1 Phenyl Isatin," *Optik (Stuttg).*, vol. 182, pp. 1211–1227, 2019, doi: https://doi.org/10.1016/j.ijleo.2019.02.010.

[17] J. H. Marin, M. L. A. Temperini, and R. A. Ando, "SERS and resonance Raman of 5-nitroisatin on silver–The distinction between the coordination and surface complexes," *Spectrochim. Acta Part A Mol. Biomol. Spectrosc.*, vol. 263, p. 120163, 2021.

[18] S. T. Hazeldine *et al.*, "Part 3: Synthesis and biological evaluation of some analogs of the antitumor agents, 2-{4-[(7-chloro-2-quinoxalinyl)oxy]phenoxy}propionic acid, and 2-{4-[(7-bromo-2-quinolinyl)oxy]phenoxy}propionic acid," *Bioorg. Med. Chem.*, vol. 13, no. 4, pp. 1069–1081, 2005, doi: https://doi.org/10.1016/j.bmc.2004.11.034.

[19] M. J. Frisch, "gaussian09," *http//www. gaussian. com/*, 2009.

[20] M. H. Jamróz, "Vibrational energy distribution analysis (VEDA): scopes and limitations," *Spectrochim. Acta Part A Mol. Biomol. Spectrosc.*, vol. 114, pp. 220–230, 2013.

[21] S. Bugalia *et al.*, "Review on Isatin- A Remarkable Scaffold for Designing Potential Therapeutic Complexes and Its Macrocyclic Complexes with Transition Metals," *J. Inorg. Organomet. Polym. Mater.*, vol. 33, no. 7, pp. 1782–1801, 2023, doi: 10.1007/s10904-023-02666-0.

[22] S. J. HOLT, "Studies in enzyme cytochemistry II. Synthesis of indigogenic substrates for ester as es," 1958.

[23] A. Bigotto and V. Galasso, "Infrared and Raman spectra of phthalimide and isatin," *Spectrochim. Acta Part A Mol. Spectrosc.*, vol. 35, no. 7, pp. 725–732, 1979, doi: https://doi.org/10.1016/0584-8539(79)80029-X.

[24] M. Govindarajan, K. Ganasan, S. Periandy, S. Mohan, and F. Tedlamelekot, "Vibrational spectroscopic analysis of 2-bromobenzoic and anthranilic acids: A combined experimental and theoretical study," *Spectrochim. Acta Part A Mol. Biomol. Spectrosc.*, vol. 79, no. 5, pp. 2003–2011, 2011, doi: https://doi.org/10.1016/j.saa.2011.06.001.

[25] J. Priscilla, D.A. Dhas, I.H. Joe, and S. Balachandran, Spectroscopic (FT-IR, FT-Raman) investigation, topological (QTAIM, RDG, ELF) analysis, drug-likeness and anti-inflammatory activity study on 2-methylaminobenzoic acid alkaloid. *Journal of Molecular Structure*, vol.*1273*, p.134261, 2023, doi.org/10.1016/j.molstruc.2022.134261.

[26] A. Lautié, D. Aslanian, M. Balkanski, J.-C. Merlin, and A. Dupaix, "Non-enzymatic hydrolysis of acetylcholine studied by Raman spectrometry," *J. Raman Spectrosc.*, vol. 7, no. 6, pp. 337–340, Dec. 1978, doi: https://doi.org/10.1002/jrs.1250070610.

[27] M. Karakaya and F. Ucun, "Spectral analysis of acetylcholine halides by density functional theory calculations," *J. Struct. Chem.*, vol. 54, pp. 321–331, 2013.

[28] B. Hernández, P. Houzé, F. Pflüger, S. G. Kruglik, and M. Ghomi, "Raman scattering-based multiconformational analysis for probing the structural differences between acetylcholine and acetylthiocholine," *J. Pharm. Biomed. Anal.*, vol. 138, pp. 54–62, 2017.